

Al₁₃H⁻: Hydrogen atom site selectivity and the shell modelA. Grubisic,¹ X. Li,¹ S. T. Stokes,¹ K. Vetter,¹ G. F. Ganteför,^{1,a),b)} K. H. Bowen,^{1,a),c)} P. Jena,^{2,a)} B. Kiran,^{3,a)} R. Burgert,⁴ and H. Schnöckel^{4,a)}¹*Department of Chemistry and Department of Materials Science, Johns Hopkins University, Baltimore, Maryland 21218, USA*²*Department of Physics, Virginia Commonwealth University, Richmond, Virginia 23284, USA*³*Department of Chemistry, McNeese State University, Lake Charles, Louisiana 70609, USA*⁴*Institute for Inorganic Chemistry, Karlsruhe University (TH), 76128 Karlsruhe, Germany*

(Received 22 January 2007; accepted 1 September 2009; published online 25 September 2009)

Using a combination of anion photoelectron spectroscopy and density functional theory calculations, we explored the influence of the shell model on H atom site selectivity in Al₁₃H⁻. Photoelectron spectra revealed that Al₁₃H⁻ has two anionic isomers and for both of them provided vertical detachment energies (VDEs). Theoretical calculations found that the structures of these anionic isomers differ by the position of the hydrogen atom. In one, the hydrogen atom is radially bonded, while in the other, hydrogen caps a triangular face. VDEs for both anionic isomers as well as other energetic relationships were also calculated. Comparison of the measured versus calculated VDE values permitted the structure of each isomer to be confirmed and correlated with its observed photoelectron spectrum. Shell model, electron-counting considerations correctly predicted the relative stabilities of the anionic isomers and identified the stable structure of neutral Al₁₃H. © 2009 American Institute of Physics. [doi:10.1063/1.3234363]

Aluminum hydride cluster anions were first studied almost a decade ago,^{1,2} and since then, the interaction of molecular hydrogen with aluminum cluster anions has also been investigated.³ Even more recently, we explored the bonding and structure of a wide variety of aluminum hydride clusters, Al_mH_n⁻, by utilizing a combination of negative ion photoelectron spectroscopy to study their anions, Al_mH_n⁻, and density functional theory calculations to characterize both their anions and their neutrals.^{4,5} The neutral counterparts of several of these anions were found to exhibit significant stability, as evidenced by their large highest occupied molecular orbital–lowest unoccupied molecular orbital (HOMO–LUMO) gaps. Their geometric structures were found to obey the predictions of the Wade–Mingos electron-counting rules, in agreement with calculations that also replicated key photoelectron-derived values. As a result, many of these hydrides were seen to be somewhat analogous in their structures and bonding to the boranes.

In aluminum hydrides, each hydrogen atom has two bonding options. It can form a single (terminal) bond with an aluminum partner, e.g., –Al–H, or it can form a bridging bond with its aluminum partners, e.g., –Al/H\Al–. Thus, in aluminum hydrides with one hydrogen atom, the lone hydrogen has two bonding choices, each of which leads to separate geometric isomers, i.e., one with a terminally (radially) bonded hydrogen atom and the other with a bridging hydrogen atom. The species, Al₁₃H, and its anion, Al₁₃H⁻, are single hydrogen atom, aluminum

hydride clusters for which the aluminum frameworks of both isomers are known (from our calculations) to have slightly distorted icosahedral symmetries. Moreover, the bare Al₁₃⁻ anion is a perfect icosahedron, and with its 40 largely delocalized valence electrons and high stability, it is emblematic of a jelliumlike shell model cluster system.⁶ Thus, because shell model concepts are applicable to it and because its lone hydrogen atom has only two bonding choices, Al₁₃H⁻ is an ideal testbed for investigating the role of the shell model in directing H atom site selectivity.

Here, we present results from our study of the Al₁₃H⁻ anion and its two possible isomers. As in our previous work on aluminum hydride cluster systems, this study relied on the synergistic application of anion photoelectron (photodetachment) spectroscopy and density functional theory calculations. The experimental sample was a beam of mass-selected Al₁₃H⁻ anions; these were “connected” to their corresponding neutrals, Al₁₃H, through the electron photodetachment process; and theoretical calculations provided structures and energetics for both anion isomers and for the global minimum of their corresponding neutral.

Anion photoelectron spectroscopy is conducted by crossing a mass-selected beam of negative ions with a fixed-frequency photon beam and energy analyzing the resultant photodetached electrons. It is governed by the energy-conserving relationship, $h\nu = \text{EBE} + \text{EKE}$, where $h\nu$ is the photon energy, EBE is the electron binding (transition) energy, and EKE is the electron kinetic energy. Briefly, our apparatus which has been described previously⁷ consists of a pulsed arc discharge source (PACIS),^{1,8} a time-of-flight mass spectrometer for mass analysis and mass selection, a neodymium-doped yttrium aluminum garnet (Nd:YAG) laser operating at 4.66 eV for photodetachment, and a magnetic

^{a)}Authors to whom correspondence should be addressed.^{b)}Also at Department of Physics, University of Konstanz, 78457 Konstanz, Germany.^{c)}Electronic mail: kbowen@jhu.edu.

bottle electron energy analyzer. In a PACIS, a discharge is struck between an anode and a grounded, metallic sample cathode as helium gas from a pulsed valve flows through the discharge region. When an extender (flow) tube is added to this arrangement, additional gases can be added downstream. In the present study, the sample electrode was aluminum, and hydrogen gas was backfilled prior to each discharge event. Upon initiation of the pulsed discharge, a plasma containing hydrogen atoms (the latter formed by the dissociation of H_2) expanded down the extender tube, cooling, clustering, and reacting along the way. The resulting anions were then subjected to extraction and mass analysis/selection. Electronic structure calculations were conducted at the density functional theory–generalized gradient approximation level using a PerdewWang91 exchange–correlation functional with triple zeta valence polarization basis sets.^{9,10} Geometries were optimized without symmetry constraints and frequency analysis was performed to assess the nature of the stationary points.

The photoelectron spectrum of $Al_{13}H^-$ had originally been measured by Burkart *et al.*,¹ and it is shown in Fig. 1(a). In that work, $Al_{13}H^-$ was generated in a PACIS, mass selected with a time-of-flight mass spectrometer, photodetached with 4.66 eV photons from a Nd:YAG laser, and its photoelectrons energy analyzed with a magnetic bottle electron spectrometer. Thus, for all practical purposes, the methods used in those experiments and in the present experiments are the same. Three major spectral peaks are apparent in the earlier work of Burkart *et al.* [Fig. 1(a)], one centered at an EBE of 2.2 eV, another at EBE=3.8 eV, and a third one at EBE=4.3 eV. For the purposes of this discussion, we have labeled the two peaks of interest here, i.e., the two lower EBE peaks in Fig. 1(a), each with letter A. As discussed by Burkart *et al.*, the 1.4–1.6 eV energy splitting between these peaks is an estimate of the HOMO-LUMO gap in neutral $Al_{13}H$, and such a large value implies that neutral $Al_{13}H$ is quite stable. This is consistent with $Al_{13}H$ having 40 valence electrons which makes it a closed shell in the jelliumlike shell model. Calculations carried out by Burkart *et al.*¹ as part of their study found the bonding between hydrogen and the aluminum framework to be covalent.

The $Al_{13}H^-$ photoelectron spectra shown in Figs. 1(b) and 1(c) were measured in the present study. The spectrum in Fig. 1(b) again exhibits three major peaks. The lowest EBE peak in this case, however, is located at EBE=3.15 eV, considerably higher in energy than the lowest EBE peak in Fig. 1(a). The next higher EBE peak in Fig. 1(b) sits at an EBE of 3.80 eV, essentially the same EBE as the second highest EBE peak in Fig. 1(a). The third peak sits at an EBE of 4.4 eV. We have labeled each of the two lower EBE peaks in this spectrum with letter B. The splitting between these two peaks is ~ 0.6 eV, considerably smaller than that between the two A peaks in Fig. 1(a). Clearly, the spectra seen in Figs. 1(a) and 1(b) are different even though they purport to be measuring the photoelectron spectrum of the same species, $Al_{13}H^-$. The reason for the difference resides in the subtleties of the PACIS conditions. This becomes evident when, upon changing the PACIS conditions, the photoelectron spectrum shown in Fig. 1(c) is observed. This spectrum exhibits both the lowest EBE peak seen in Fig. 1(a) and the lowest EBE peak seen in

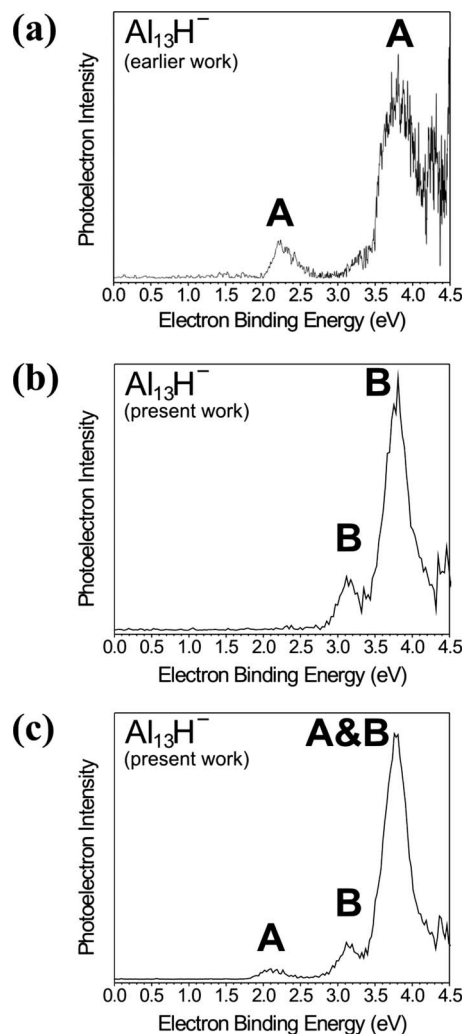


FIG. 1. (a) The photoelectron spectrum of $Al_{13}H^-$ recorded by Burkart *et al.* in their earlier work (Ref. 1). The peaks labeled with letter A are the spectral signature of isomer A. (b) A photoelectron spectrum of $Al_{13}H^-$ measured in the present work. The peaks labeled with letter B are the spectral signature of isomer B. (c) A photoelectron spectrum of $Al_{13}H^-$ recorded in the present work but under different source conditions from that in (b). It shows the presence of both isomers A and B in a single spectrum. In all of these spectra, $Al_{13}H^-$ anions were generated using a PACIS, and photodetachment was accomplished with 4.66 eV photons.

Fig. 1(b), along with a composite peak at the common location of the second highest EBE peaks seen in both Figs. 1(a) and 1(b) and a composite peak for the third highest EBE peaks seen in both spectra. Thus, the changes observed in these spectra under different source conditions imply that there are *two viable isomers* of the $Al_{13}H^-$ anion, isomer A and isomer B.

In an effort to delineate the major factor(s) influencing the preference of one isomer over the other, a series of control experiments was conducted.¹¹ From these experiments, the timing delay between the arc discharge and the ion extraction emerged as the critical parameter determining the relative ratios of the two isomers. In particular, it was found that with longer delays, isomer B became more prominent among the two, whereas isomer A was only observed at shorter delays. The result suggests that isomer A is a metastable species with a lifetime on the order of the time scale of

the experiment (several tens of microseconds), whereas isomer B is likely the thermodynamically more stable isomer. This interpretation is consistent with the observation that isomer B is present regardless of the circumstances, whereas isomer A exists only under a certain set of conditions. Note that the previously unassigned shoulder in the energy range from 3.0 to 3.5 eV in Fig. 1(a) is likely due to isomer B, already present in small amounts in those earlier experiments.

The lowest EBE peaks in Figs. 1(a) and 1(b) provide measurements of the vertical detachment energies (VDEs) for their respective Al_{13}H^- anionic isomers. The VDE is the EBE value of the intensity maximum in the lowest EBE peak, representing the maximum Franck–Condon overlap in the essentially instantaneous transition from the ground state of the anion to the ground state of its corresponding neutral. The VDE thus represents the energy difference between the anion in its equilibrium structure and the anion's neutral counterpart in that same structure. VDE values are therefore well-defined quantities which can be extracted from photoelectron spectra with relative confidence. Thus, for isomer A, $\text{VDE}=2.2$ eV, while for isomer B, $\text{VDE}=3.15$ eV.

Because Al_{13}H^- has one hydrogen atom, only two viable exocage isomers are possible. Our calculations found minima on the potential surfaces of the terminal H atom isomer of anionic Al_{13}H^- and the bridging H atom isomer of anionic Al_{13}H^- . In terms of relative energies, our calculations found the terminal H atom isomer of anionic Al_{13}H^- to have a lower total energy than the bridging H atom isomer of anionic Al_{13}H^- . VDEs were calculated to be 2.26 and 3.18 eV for the bridged and the terminal H atom isomers, respectively, and they agreed well with our two experimentally determined values. Thus, by comparing measured and calculated VDE values, isomer A is seen to be the Al_{13}H^- isomer with a bridging H atom, while isomer B is identified as the Al_{13}H^- isomer with a terminal H atom. This is consistent with our experimentally based hypothesis that anionic isomer B is more stable than anionic isomer A since our calculations show that the terminal H atom anionic isomer is the more stable of the two, and anionic isomer B is now seen to be that isomer.

On the potential energy surface of neutral Al_{13}H , the bridging H atom structure was found to be a minimum. Because the anionic bridging H atom structure is a minimum as well, an EA_a value is well defined. It was calculated to be 1.99 eV. Knowing now that the bridging H atom isomer is isomer A, we can estimate its EA_a value from the low EBE side of isomer A's lowest EBE peak. This value is ~ 2.0 eV, and it is in good agreement with the calculated value. On the other hand, the neutral Al_{13}H structure resembling that of the terminal H atom isomer of anionic Al_{13}H^- was not found to be a minimum, corresponding instead to a second order saddle point. Following the path of imaginary frequencies led to the bridging H atom structure of neutral Al_{13}H , i.e., neutral Al_{13}H 's global minimum.

Figure 2 shows the calculated energetics and structures of both anionic isomers and their corresponding neutrals. While all 12 aluminum atoms that make up the shell of icosahedral Al_{13}^- are structurally equivalent, when a hydro-

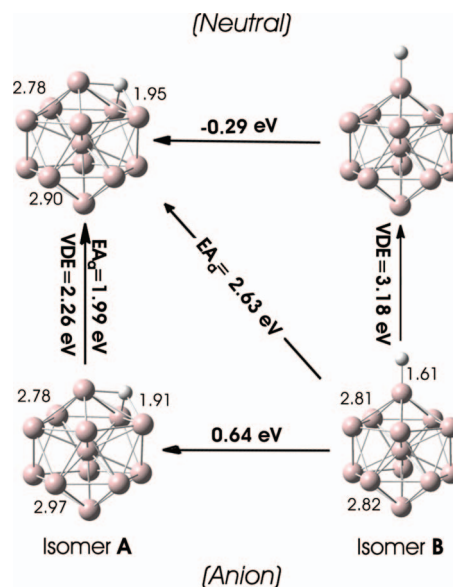


FIG. 2. Calculated lowest energy structures of both isomers of anionic Al_{13}H^- and neutral Al_{13}H along with their calculated energetic relationships.

gen atom bonds to its cage in either a terminal or a bridged motif, the aluminum framework undergoes a distortion away from perfect icosahedral symmetry. Of particular interest, one sees that the hydrogen atom in both the anion and the neutral of isomer A bridges across three aluminum atoms (a face), whereas in Al_4H_6 (D_{2d}), for example, the two bridging H atoms each link across two aluminum atoms.⁴

Figure 3 schematically depicts the main transitions (and their energies) in the photoelectron spectra along with various calculated energetic values. This figure further illustrates

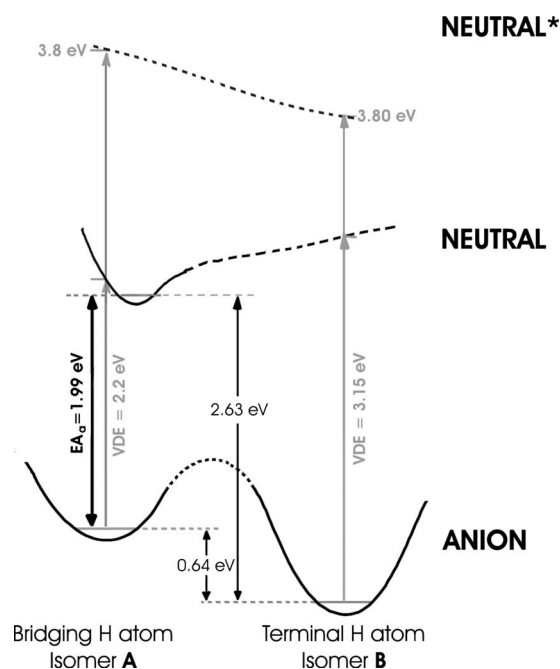


FIG. 3. Schematic representation of the photodetachment transitions between both isomers of Al_{13}H^- anions and their corresponding Al_{13}H neutral forms. Both experimentally measured (gray) and theoretically computed (black) energetic values are shown. (The asterisk “*” signifies the first electronically excited state of neutral Al_{13}H .)

that the bridging H atom structure is neutral Al_{13}H 's global minimum, while among Al_{13}H^- anions, the terminal H atom isomer (B) possesses the lower energy. Furthermore, the calculated energy difference between the most stable Al_{13}H^- anion (the terminal H atom structure, isomer B) and the most stable neutral Al_{13}H (the bridging H atom structure) was calculated to be 2.63 eV, i.e., the thermodynamic electron affinity of the Al_{13}H system. Since photodetachment transitions are "vertical," connecting an anion of a given structure to its neutral counterpart with the same instantaneous structure, one should not observe a transition from the terminal H atom structure of anionic Al_{13}H^- (isomer B) to the bridging H atom structure of neutral Al_{13}H in the photoelectron spectrum of anionic isomer B [Fig. 1(b)]. As expected, there is no significant photoelectron intensity at $\text{EBE} \approx 2.6$ eV. (The nearby peak centered at $\text{EBE} = 3.15$ eV is well assigned to a different transition.)

Aluminum is a good free electron metal and the electronic structures of aluminum clusters such as Al_{13}^- are well known to be governed by the jelliumlike shell model. In an aluminum-rich species, such as Al_{13}H^- , it is natural to wonder whether H atom site selectivity is also influenced by the shell model's propensity for forming closed shells with specific numbers of valence electrons. For a cluster composed of 13 aluminum atoms, as in the present case, the proximate shell closing number of valence electrons occurs at 40 valence electrons, e.g., Al_{13}^- has 40 valence electrons and is very stable. Adding one more electron to make a total of 41 electrons causes a relative destabilization of such a system because the next available (empty) energy level is well above the (stabilized) level that is home to the 39th and 40th electrons of the closed shell.

In considering the stability of a cluster anion in terms of the shell model, only those valence electrons that contribute to the stability of the system through delocalization should be counted. In the case of Al_{13}H^- , this puts the focus on the aluminum metal atom cage. In the terminal H atom motif, the Al-H bond utilizes two electrons which become localized and, consequently, cannot contribute to delocalization in the aluminum cage, whereas in the bridging H atom motif, the hydrogen atom effectively donates its electron to the cage by forming a delocalized bond with its aluminum neighbors. Thus, for anionic isomer A with its bridging H atom, the cage has $3 \times 13 = 39$ electrons available from the aluminum atoms, plus 1 electron from the bridged hydrogen atom, plus 1 electron due to Al_{13}H^- 's negative charge, summing to 41 total electrons. With 1 electron more than the closed shell at 40 electrons, anionic isomer A is thus expected to suffer some degree of destabilization. By contrast, anionic isomer B with its terminal H atom has 39 electrons available from the aluminum atoms, plus 1 electron from the hydrogen atom, plus 1 electron from the net negative charge, minus 2 electrons that are tied up in the localized Al-H terminal bond, totaling to 39 electrons. While this is 1 electron less than the 40 needed to close the shell, 1 less than 40 (for anionic isomer B) is not the same as 1 more than 40 (as in the case of anionic isomer A). With its 39 electrons, anionic isomer B

has gathered significant stability since it has half-filled the shell closing level. Some time ago, we saw this behavior in the case of magnesium cluster anions, where Mg_{19}^- , with its 39 valence electrons, exhibited a dramatically enhanced ion intensity in the mass spectrum of Mg_n^- , i.e., it was a magic number species, while the intensity of Mg_{20}^- , with its 41 valence electrons, plunged toward the base line.¹² Thus, the shell model predicts that anionic isomer B should be relatively more stable than anionic isomer A, substantiating both our experimental and our theoretical findings. Furthermore, the shell model also predicts that the bridging H atom structure of neutral Al_{13}H , with its 40 valence electrons, should be more stable than a terminal H atom structure of neutral Al_{13}H , with its 38 valence electrons, again corroborating our theoretical results. This is also consistent with the observed relatively large HOMO-LUMO gap of the bridging H atom structure of neutral Al_{13}H that can be inferred from the photoelectron spectrum of isomer A [Fig. 1(a)].

It seems clear that H atom site selectivity in Al_{13}H^- and in Al_{13}H is significantly influenced, if not governed, by shell model considerations. In future work, we will explore the influence of the shell model on H atom site selectivity in more complex, metal-rich aluminum hydride cluster anions. For a subset of such systems, a strong correlation between sites that a hydrogen atom prefers to bind to and the attainment of a closed shell within the resulting structures was indeed recently observed, supporting the conclusions reached in this report.¹³

This work was supported by the (U.S) Air Force Office of Scientific Research (K.H.B.), by the Department of Energy (P.J.), and by the Deutsche Forschungsgemeinschaft (G.F.G. and H.S.).

¹S. Burkart, N. Blessing, B. Klipp, J. Miller, G. Ganteför, and G. Seifert, *Chem. Phys. Lett.* **301**, 546 (1999).

²B. K. Rao, P. Jena, S. Burkart, G. Ganteför, and G. Seifert, *Phys. Rev. Lett.* **86**, 692 (2001).

³L.-F. Cui, X. Li, and L.-S. Wang, *J. Chem. Phys.* **124**, 054308 (2006).

⁴X. Li, A. Grubisic, S. T. Stokes, J. Cordes, G. F. Ganteför, K. H. Bowen, B. Kiran, M. Willis, P. Jena, R. Burgert, and H. Schnöckel, *Science*, **315**, 356 (2007).

⁵A. Grubisic, X. Li, S. T. Stokes, J. Cordes, G. F. Ganteför, K. H. Bowen, B. Kiran, P. Jena, R. Burgert, and H. Schnöckel, *J. Am. Chem. Soc.* **129**, 5969 (2007).

⁶R. E. Leuchtner, A. C. Harms, and A. W. Castleman, Jr., *J. Chem. Phys.* **91**, 2753 (1989).

⁷M. Gerhards, W.-J. Zheng, O. C. Thomas, T. Lippa, S.-J. Xu, and K. H. Bowen, *J. Chem. Phys.* **124**, 144304 (2002).

⁸H. R. Siekmann, C. Lueder, J. Faehrmann, H. O. Lutz, and K. H. Meiwes-Broer, *Z. Phys. D: At., Mol. Clusters* **20**, 417 (1991).

⁹All calculations were done using GAUSSIAN 03 software, Revision C.02, M. J. Frisch, G. W. Trucks, H. B. Schlegel *et al.*, Gaussian, Inc., Wallingford, CT, 2004.

¹⁰R. Ahlrichs and S. D. Elliott, *Phys. Chem. Phys. Chem.* **1**, 13 (1999).

¹¹See EPAPS supplementary material at <http://dx.doi.org/10.1063/1.3234363> for results of a series of control experiments.

¹²O. C. Thomas, W.-J. Zheng, S.-J. Xu, and K. H. Bowen, *Phys. Rev. Lett.* **89**, 213403 (2002).

¹³B. Kiran, P. Jena, X. Li, A. Grubisic, S. T. Stokes, G. F. Ganteför, K. H. Bowen, R. Burgert, and H. Schnöckel, *Phys. Rev. Lett.* **98**, 256802 (2007).